

Observation of coupled vortex gyrations by 70-ps-time- and 20-nm-space-resolved full-field magnetic transmission soft x-ray microscopy

Hyunsung Jung,¹ Young-Sang Yu,¹ Ki-Suk Lee,¹ Mi-Young Im,² Peter Fischer,²
Lars Bocklage, Andreas Vogel,³ Markus Bolte,³ Guido Meier,³ and Sang-Koog Kim^{1,a)}

¹Research Center for Spin Dynamics and Spin-Wave Devices, and Nanospinics Laboratory,
Department of Materials Science and Engineering, Seoul National University, Seoul 151-744,
Republic of Korea

²Center for X-ray Optics, Lawrence Berkeley National Laboratory, Berkeley, California 94720, USA

³Institut für Angewandte Physik und Zentrum für Mikrostrukturforschung, Universität Hamburg,
Hamburg 20355, Germany

We employed time- and space-resolved full-field magnetic transmission soft x-ray microscopy to observe vortex-core gyrations in a pair of dipolar-coupled vortex-state Permalloy (Ni80Fe20) disks. The 70 ps temporal and 20 nm spatial resolution of the microscope enabled us to simultaneously measure vortex gyrations in both disks and to resolve the phases and amplitudes of both vortex-core positions. We observed their correlation for a specific vortex-state configuration. This work provides a robust and direct method of studying vortex gyrations in dipolar-coupled vortex oscillators. © 2010 American Institute of Physics. [doi:10.1063/1.3517496]

Recently, vortex-core oscillations in micrometer-size (or less) magnetic elements have been intensively studied for their promising application as microwave emission sources.^{1–12} Vortex-core oscillators provide high-power output and narrow linewidths. Most studies have focused on electrical measurements using isolated single disks.^{4,10–12} However, the need for high-power signals and high packing density have spurred further studies, not only on coupled vortex-state disks but also on multiple-disk arrays. In cases of sufficiently short distances between nearest neighboring disks, dipolar interaction alters their dynamics.^{13–15} Thus, the examination of the influence of dipolar interaction on vortex oscillations is important. To characterize the interaction between individual elements a time- and space-resolving measurement technique is mandatory.

Recent advances in time-resolved microscopy enable imaging of the spin dynamics of nanoscale magnetic elements at a time resolution of less than 100 ps.^{16,17} Time-resolved full field imaging is required for simultaneous measurement of different local areas. In this letter, we chose a pair of physically separated disks in order to resolve vortex gyrations in both disks, along with their amplitude and phase relations. We report on an experimental observation of coupled vortex gyrations in Permalloy (Py: Ni80Fe20) disks and the effect of dipolar interaction on each disk's gyration.

The two-disk system studied was prepared on a 100-nm-thick silicon nitride membrane by electron-beam lithography, thermal evaporation, and lift-off processing. Each Py disk has a diameter of $2R = 2.4 \text{ }\mu\text{m}$ and a thickness of $L = 50 \text{ nm}$. The disks are arranged in a pair with a center-to-center distance of $d_{\text{int}} = 2.52 \text{ }\mu\text{m}$ (see Fig. 1). In order to locally excite one vortex, a 1.5- μm -wide and 75-nm-thick Cu strip covers the top of the right Py disk, as can be seen in Fig. 1. The vortex eigenfrequency of around $157 \pm 3 \text{ MHz}$ in the isolated Py disks was measured on an array of Py disk pairs of identical dimensions¹⁸ using a broadband-ferromagnetic resonance setup.¹⁵

Measurements of the dynamic evolution of vortex-core gyrations were carried out by full-field magnetic transmission soft x-ray microscopy (MTXM) at beamline 6.1.2, Advanced Light Source (ALS), Berkeley, CA, utilizing a stroboscopic pump-and-probe technique. The optical setup of the x-ray microscope,¹⁹ shown in Fig. 2, consists of the bending magnet source providing elliptically polarized soft x rays, a monochromator and illuminating assembly (comprising the first Fresnel zone plate, the condenser zone plate, and a pinhole close to the sample), a high resolution imaging objective lens, the microzone plate, and a two-dimensional charge coupled device (CCD) detector. The spatial resolution is mainly determined by the outermost zone width of the microzone plate. The temporal resolution is set by the inherent pulsed time structure of the x-ray source, and is typically about 70 ps in two-bunch mode operation of the ALS, where two electron bunches of 70 ps length are separated by 328 ns.^{20,21} The magnetization contrasts of the Py disks in the present study were measured by monitoring the spatial distribution of the local magnetizations through x-ray magnetic

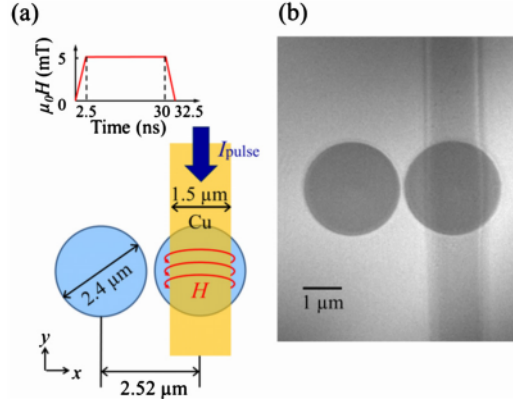


FIG. 1. (Color online) Schematic illustration of two-disk system and its structural transmission soft x-ray image.

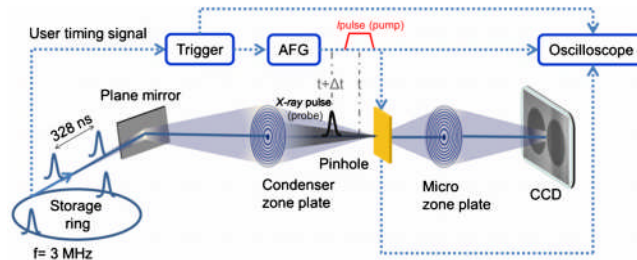


FIG. 2. (Color online) Schematic of the full-field magnetic transmission soft x-ray microscope at beamline 6.1.2, and an illustration of the stroboscopic pump-and-probe technique including the arbitrary function generator (AFG) and the soft x-ray sensitive CCD camera.

circular dichroism (XMCD) at the Fe L_3 absorption edge (here -707 eV). To be sensitive to the in-plane component of the magnetization, the sample surface was positioned at 60° orientation to the propagation direction of the incident x rays.

The clock signal of the synchrotron triggers an arbitrary function generator (Agilent, 81150A), which launches particular pulses into a strip line. These pump pulses create local Oersted fields. Field pulses of 5 mT strength, 30 ns length, and 2.5 ns rise and fall time were stroboscopically applied along the x axis on which the two disks were placed [see Fig. 1(a)]. The driving pulses were synchronized with x-ray probe pulses to a frequency of -3 MHz. To measure the temporal evolution of the vortex excitations, the pulses were delayed with respect to the x-ray probe pulse. The arrival time of the x-ray pulses at the sample was monitored by a fast avalanche photodiode.²¹ In order to obtain sufficient XMCD contrasts, ten individual images of several million accumulated x-ray flashes measured at the identical time delay, were integrated. The x-ray images were recorded at every 1.67 ns step.

Figure 3 shows the resultant plane-view data for both disks as measured after a perturbation of the right disk by the pulse field. In the images, the structural contrast is normalized by an image obtained under a static saturation field. The relatively bright region in the disks represents magnetizations that point in the $+x$ direction, whereas the relatively dark area corresponds to opposite-direction magnetizations. Both disks' initial configuration shows the same chirality of clockwise in-plane curling magnetization, $C_1 = C_2 = -1$. The core polarization can be determined from the sense of rotation of the cores after excitation.^{1,5} The upward core in disk 1 gyrates counterclockwise, indicating $p_1 = +1$, whereas the downward core in disk 2 gyrates clockwise, corresponding to $p_2 = -1$ (see the top of each column in Fig. 3).

In the serial images, the core positions of both disks can be determined by the variations of the in-plane curling magnetizations. The vortex-core oscillation around its center position in disk 1 (right disk) is excited by the local field of the strip line at the beginning of perturbation. The vortex gyration in disk 2, also shown in Fig. 3, is not excited by the local field, but is induced by the dipolar interaction with its neigh-

boring disk. Local fields produced through the Cu strip did not excite the neighboring disk, which is proven by experimental confirmation with a reference sample that contained only the disk beside the strip. Calculations also confirm that the local fields emanating from the strip line can be neglected at the position of the left disk.²² The core positions varying in time and in in-plane space over a relatively large area are resolved in both disks. Correlations of the amplitudes and phases of both vortex-core positions can be easily identified with reference to the serial images.

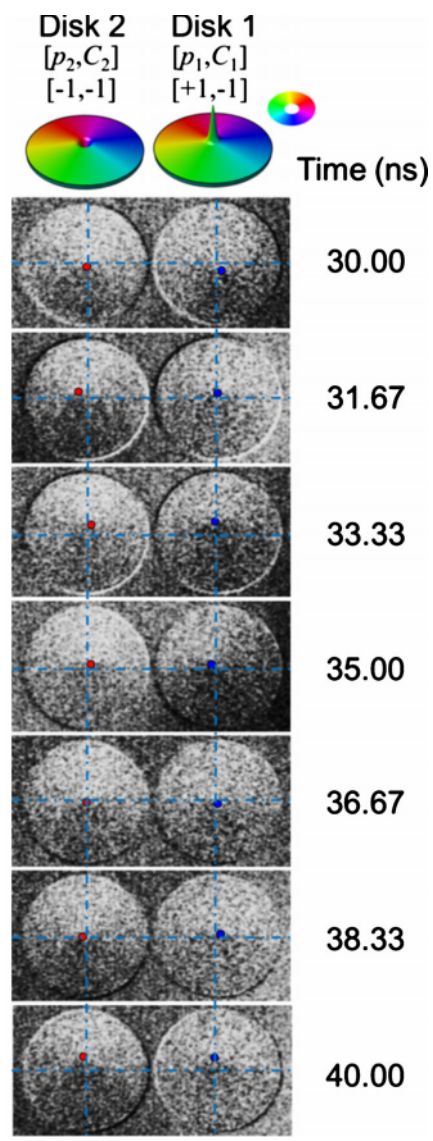


FIG. 3. (Color online) XMCD images of the dynamic evolution of vortex gyrotropic motions in both disks, and corresponding vortex states represented by color and height of the surface: $p_1 = +1$, $p_2 = -1$, and $C_1 = C_2 = -1$. The dotted vertical and horizontal lines indicate the center position of each disk.

According to the vortex-core positions that evolve over time, the x and y components are plotted as functions of time in Fig. 4(a). The components provide information about the correlations of the core orbit amplitudes and phases between the two gyrations. The x components in both disks show out-of-phase oscillations, whereas the y components show in-phase ones, during the relaxation process after the short pulse field is turned off. The amplitudes of both core oscillations decrease due to their damping. The anti-phase relation along the x axis and the in-phase relation along the y axis reflect the core polarizations and the chiralities of both disks. The initial motion of the vortex core under the strip line is caused by the field pulse, and depending on the chirality the vortex core moves in the positive or

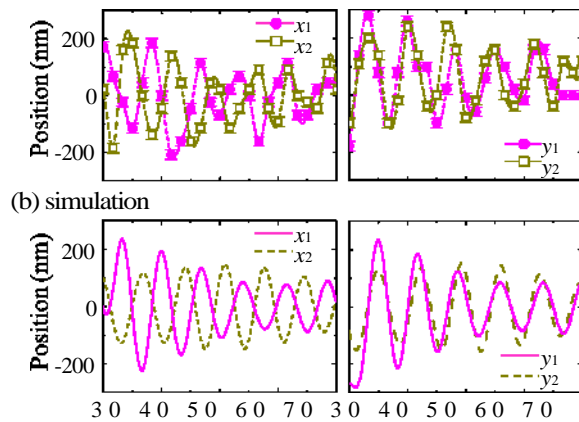


FIG. 4. (Color online) Oscillations of the x and y components of both vortex-core positions as function of time. (a) MTXM measurement results. The dashed lines were drawn using spline interpolation. (b) Micromagnetic simulation results for the same geometry and pulse parameters as those in the experiment.

negative y direction. The sense of core rotation is determined by the polarization p . The relative core positions change the effective stray field of each disk. The

experimental results were confirmed to be in quantitative agreement with the simulation results²³ for the same geometry and pulse parameters [shown in Fig. 4(b)]. The estimated eigenfrequency from the vortex-core oscillations shown in Fig. 4(a) is about 143 ± 14 MHz, which equals to the value obtained from the simulation. The uncertainty of the core position in Fig. 4(a) was about 33 nm, considering both the spatial and time resolutions of the measurement.

We want to emphasize, that the vortex-core gyration in disk 2 was stimulated by the stray field of the neighboring disk 1 that varies with the position of the vortex core. Energy transfer between separate disks by dipolar-induced gyration is possible. It would be interesting for the purposes of a future study to examine gyrations for different d_{nt} and their vortex-state-configuration dependence.

In summary, we employed 70-ps-time- and 20-nmspace-resolved, full-field magnetic transmission soft x-ray microscopy to simultaneously measure vortex-core positions in separated disks. The unique capabilities of time-resolved full field magnetic soft x-ray microscopy allowed us to unambiguously resolve the individual vortex gyrations in both disks and to directly study their interaction. It was found that the vortex gyration of one disk affects that of the other through dipolar interaction. We investigated coupled vortex- state disks of the same clockwise in-plane curling magnetization and antiparallel core orientations. For this configuration, we observed out-of-phase (in-phase) oscillations of the vortex-core positions along the x axis (y axis). This work provides a robust and direct method of studying the dynamics of vortex gyrations and dipolar interaction in spatially separated disks.

Note added in proof. During its review process, we became aware of a recent publication on gyration mode splitting in magnetostatically coupled magnetic vortices studied by time-resolved magneto-optical Kerr effect (Ref. 24).

This work was supported by the Basic Science Research Program through the National Research Foundation of Korea

Funded by the Ministry of Education, Science and Technology (Grant No. 20100000706). The operation of the microscope was supported by the Director, Office of Science, Office of Basic Energy Sciences, Materials Sciences and Engineering Division of the U.S. Department of Energy under DE-AC02-05-CH11231. Financial support of the Deutsche Forschungsgemeinschaft via the SFB 668 "Magnetismus vom Einzelatom zur Nanostruktur," and via the Graduiertenkolleg 1286 "Functional Metal-Semiconductor Hybrid Systems" as well as by the City of Hamburg via Cluster of Excellence "Nano-Spintronics" is gratefully acknowledged.

¹K. Y. Guslienko, B. A. Ivanov, V. Novosad, H. Shima, Y. Otani, and K. Fukamichi, *J. Appl. Phys.* **91**, 8037 (2002).

²S. Kasai, Y. Nakatani, K. Kobayashi, H. Kohno, and T. Ono, *Phys. Rev. Lett.* **97**, 107204 (2006).

³K.-S. Lee and S.-K. Kim, *Appl. Phys. Lett.* **91**, 132511 (2007).

⁴V. S. Pribyag, I. N. Krivorotov, G. D. Fuchs, P. M. Braganca, O. Ozatay, J. C. Sankey, D. C. Ralph, and R. A. Buhrman, *Nat. Phys.* **3**, 498 (2007).

- ⁵K.-S. Lee and S.-K. Kim, *Phys. Rev. B* **78**, 014405 (2008).
- ⁶Y.-S. Choi, S.-K. Kim, K.-S. Lee, and Y.-S. Yu, *Appl. Phys. Lett.* **93**, 182508 (2008).
- ⁷Q. Mistral, M. van Kampen, G. Hrkac, J.-V. Kim, T. Devolder, P. Crozat, C. Chappert, L. Lagae, and T. Schrefl, *Phys. Rev. Lett.* **100**, 257201 (2008).
- ⁸Y.-S. Choi, K.-S. Lee, and S.-K. Kim, *Phys. Rev. B* **79**, 184424 (2009).
- ⁹A. Ruotolo, V. Cros, B. Georges, A. Dussaux, J. Grollier, C. Deranlot, R. Guillemet, K. Bouzehouane, S. Fusil, and A. Fert, *Nat. Nanotechnol.* **4**, 528 (2009).
- ¹⁰R. Lehdorff, D. E. Bürgler, S. Gliga, R. Hertel, P. Grünberg, C. M. Schneider, and Z. Celinski, *Phys. Rev. B* **80**, 054412 (2009).
- ¹¹G. Finocchio, V. S. Pribiag, L. Torres, R. A. Buhrman, and B. Azzerboni, *Appl. Phys. Lett.* **96**, 102508 (2010).
- ¹²A. Dussaux, B. Georges, J. Grollier, V. Cros, A. V. Khvalkovskiy, A. Fukushima, M. Konoto, H. Kubota, K. Yakushiji, S. Yuasa, K. A. Zvezdin, K. Ando, and A. Fert, *Nat. Commun.* **1**, 8 (2010).
- ¹³J. Shibata, K. Shigeto, and Y. Otani, *Phys. Rev. B* **67**, 224404 (2003).
- ¹⁴Y. Liu, H. Zhiwei, S. Gliga, and R. Hertel, *Phys. Rev. B* **79**, 104435 (2009).
- ¹⁵A. Vogel, A. Drews, T. Kamionka, M. Bolte, and G. Meier, *Phys. Rev. Lett.* **105**, 037201 (2010).
- ¹⁶A. Puzic, B. V. Waeyenberge, K. W. Chou, P. Fischer, H. Stoll, G. Schütz, T. Tyliczszak, K. Rott, H. Brühl, G. Reiss, I. Neudecker, T. Haug, M. Buess, and C. H. Back, *J. Appl. Phys.* **97**, 10E704 (2005).
- ¹⁷L. Bocklage, B. Krüger, R. Eiselt, M. Bolte, P. Fischer, and G. Meier, *Phys. Rev. B* **78**, 180405(R) (2008).
- ¹⁸For the ferromagnetic resonance measurement, an array of Py disk pairs was placed under a 7- μm -wide stripline. The disks were of the same dimensions ($2R = 2.4 \mu\text{m}$ and $L=50 \text{ nm}$), but a larger value of $d_{\text{int}}=3.74 \mu\text{m}$ was used to prevent interaction.
- ¹⁹P. Fischer, T. Eimüller, G. Schütz, G. Denbeaux, A. Lucero, L. Johnson, D. Attwood, S. Tsunashima, M. Kumazawa, N. Takagi, M. Köhler, and G. Bayreuther, *Rev. Sci. Instrum.* **72**, 2322 (2001).
- ²⁰B. L. Mesler, P. Fischer, W. Chao, E. H. Anderson, and D.-H. Kim, *J. Vac. Sci. Technol. B* **25**, 2598 (2007).
- ²¹P. Fischer, *AAPPS Bull.* **18**(6), 12 (2008).
- ²²The in-plane component of the local fields is effective only in the one disk on which the Cu electrode is placed; the out-of-plane field component is too weak to affect vortex excitations.
- ²³We used the OOMMF code. See <http://math.nist.gov/oommf>. The material parameters of the Py disks were as follows: the exchange stiffness $A_{\text{ex}} = 13 \text{ pJ/m}$ and the saturation magnetization $M_{\text{s}} = 7.2 \times 10^5 \text{ A/m}$ with a zero magnetic anisotropy constant. The cell size was $4 \times 4 \times 50 \text{ nm}^3$ with the damping constant $\alpha=0.01$.
- ²⁴A. Barman, S. Barman, T. Kimura, Y. Fukuma, and Y. Otani, *J. Phys. D*, **43**, 422001 (2010).

DISCLAIMER

This document was prepared as an account of work sponsored by the United States Government. While this document is believed to contain correct information, neither the United States Government nor any agency thereof, nor the Regents of the University of California, nor any of their employees, makes any warranty, express or implied, or assumes any legal responsibility for the accuracy, completeness, or usefulness of any information, apparatus, product, or process disclosed, or represents that its use would not infringe privately owned rights. Reference herein to any specific commercial product, process, or service by its trade name, trademark, manufacturer, or otherwise, does not necessarily constitute or imply its endorsement, recommendation, or favoring by the United States Government or any agency thereof, or the Regents of the University of California. The views and opinions of authors expressed herein do not necessarily state or reflect those of the United States Government or any agency thereof or the Regents of the University of California.